Development of Upper-extremity Exoskeleton driven by Pneumatic Cylinder toward Robotic Rehabilitation Platform for Shoulder Elevation

Tomoyuki Noda[1] and Jun Morimoto[1]

Abstract— **While many upper-extremity exoskeleton systems have been developed for rehabilitation, there are still challenges in designing an exoskeleton which has a back-drivable joint for assured safety and simultaneously can generate large assistive torque. This paper introduces a newly developed upper-extremity exoskeleton robot intended as a rehabilitation platform specialized for elevation of shoulder joint. By using a pneumatic cylinder, the shoulder joint can be back-drivable and can have hardware compliance while it fully actuates the entire arm, of both the exoskeleton and the user. In addition, our development is particularly featured in (a) the length-adjustable frame, (b) the high-resolution encoder built into a thrust bearing in a hollow compact joint, and (c) the physical slider implemented as an easy-to-use interface. We also developed a torque-based controller for the exoskeleton so that the therapist can teach the shoulder joint movement directly. In the experiment, we showed that we can program the exoskeleton robot movement by directly moving the exoskeleton with mannequin arm while the weights of the robot and the mannequin was supported using the gravity compensation control method.**

I. INTRODUCTION

An increasing number of patients require rehabilitation after suffering a stroke [1]. Designing platforms for robotic rehabilitation requires different aspects of key technologies from industrial factory automation; in particular, the actuator itself has to be back-drivable and compliant for assured safety.

In previously developed platforms, making the arm reach a target position on a horizontal plane was considered the standard target movement while the arm is balanced or stabilized on the sagittal plane. On the other hand, a system that assists with elevation of the shoulder joint angle and that maintains the user's posture on the sagittal plane prior to making the reaching motion has not been sufficiently considered. While several conventional platforms also partially assist shoulder elevation in a sagittal plane, we found that, in rehabilitation fields, there are more demands for a robotic system. It is required to substitute an elevation movement of the user's shoulder even the joint is stiff by a spasmus. Therefore, in this study, we introduce our attempt to develop a simple and lightweight upper-limb exoskeleton with assured safety specialized to assisting shoulder-joint movements with an easy-to-use interface. In exoskeleton robot design, it is also very important to provide a system that can be properly adjusted for arm length.

[1]The authors are with ATR Computational Neuroscience Laboratories, 2-2-2 Hikaridai, Seikacho, Soraku-gun, Kyoto 619-0288, Japan {t_noda,xmorimo}@atr.jp

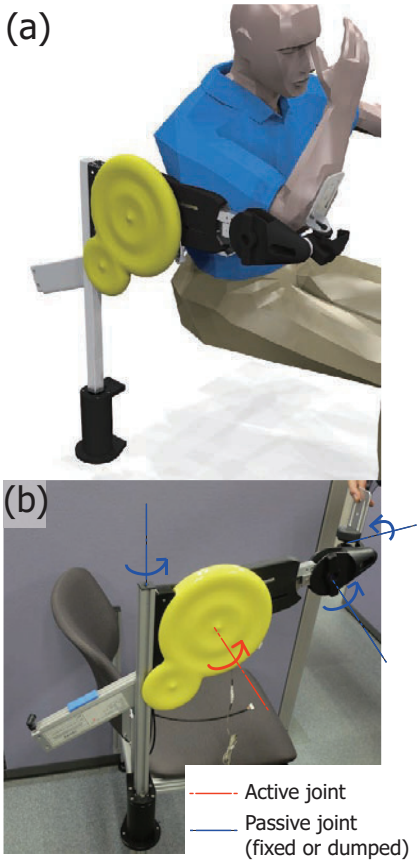

Fig. 1. Developed shoulder exoskeleton: a 1-DOF active joint for flexion-extension of shoulder and 3-DOF passive joints for adjustment.

Electric geared motors are unsuited for constructing an compact exoskeleton system for assisting shoulder-joint movements on the sagittal plane because continuously supplying constant torque to maintain a shoulder-joint posture generates a considerable amount of heat. To overcome such problem, passive weight compensation [2] or spring balancing mechanisms to lower the demands on the motors are necessary. Consequently, the inertia and the size of the exoskeleton became large. In addition, active movements against a stiff shoulder due to spasm requires large torque. The motor system need to increase the gear ratio in a compact motor, losing its back-drivability.

978-1-4799-1808-9/15/$31.00 ©2015 IEEE

To avoid this trade-off, in place of geared motors, pneumatic actuators can be utilized to achieve a soft, movement-compliant actuator [3]. In fact, compared to platforms actuated by electric geared motors [4], [5] or hydraulic cylinders[6], pneumatic actuators [7], [8], [9], [10], [11], [12] show greater promise in developing a lightweight and compliant exoskeleton with a large power/weight ratio.

Therefore, we adopt a pneumatic cylinder in our system. A similar concept can be found in the conventional platforms[8][9]. In addition, we developed a compact shoulder joint with running electric wires through the joint axis, following the "hollow wrist" design widely adopted in industrial robotics. In addition, a thrust bearing with a high-resolution built-in encoder are used for the compact shoulder design. By using a wedge structure for the link of the exoskeleton, we can easily adjust the link length of the exoskeleton without loosing rigidity. Consequently, sufficient torque can be transmitted to a user's arm via the compact exoskeleton frame actuated by a pneumatic cylinder.

In this paper, we mainly introduce the state-of-the-art in our hardware design in the following sections. In addition, we also introduce a torque-based controller with gravity compensation that can be used for learning demonstrated movements. Since the assistive robot eventually needs to be operated by a therapist, the robot's control interface should be simple and intuitive enough for an operator who is not a robotics expert. Therefore, we developed the Physical Slider Interface (PSI), which can be used to control the exoskeleton at a rehabilitation site without using a computer screen.

II. Mechatronics Design and Torque-based Controller

Figures 1 (a) and (b) show the developed upper-extremity exoskeleton. As shown in Fig. 1 (b), the exoskeleton arm is attached to a chair so that user movements can be assisted while the user is sitting. Fig. 1 (b) also shows the joint axes' arrangements. One of the four degrees of freedom (DOF) is the active joint actuated by a pneumatic cylinder. Another DOF is a passive joint that allows lateral shoulder angle adjustment. This passive joint is connected to a rotational dumper. The developed robot also has two additional DOFs at the elbow to select and fix arm posture, composed of adjustments to shoulder internal rotation and elbow flexion-extension. Since the main scope of this paper is the design around the active joint of shoulder, in following section, we mainly introduce the detailed mechatronics designs and the implementation of the torque-based controller in regard to the shoulder flexion-extension.

A. High-resolution encoder built into thrust bearing

Fig.2 shows a cross-sectional view of the shaft of the active joint for assisting shoulder flexion-extension movements, where the active joint is actuated by a pneumatic cylinder (DZF-32: Festo Co., Ltd., nominal force is 483 N at 0.6 MPa). The joint has a hollow-shaft for easy wiring. Three bearings, including two ball bearings and one thrust needle bearing, are implemented on the hollow-shaft. The angle measurement is provided by the high-resolution encoder system built into the thrust bearing. A small optical encoder (Avago Co., Ltd., AEDR-8500) is mounted on a flexible printed circuit (FPC) board, and a thin scale (1000 CPR, custom made using melt-forming technology) is implemented in the small space between the thrust bearing and the hollow axis (4mm $\times$ 5mm ring shape space). The mounter of the scale, the scale, and FPC are placed using positioning pins to control relative positions.

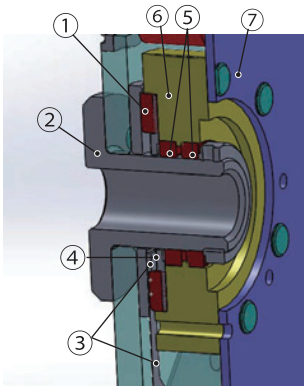

Fig. 2. Cross-sectional view of the hollow shaft with built-in optical encoder: 1) thrust bearing, 2) hollow-shaft for wiring, 3) optical encoder and FPC, 4) 1000 CPR scale mounted to a modified thrust bearing washer, 5) bearings, 6) joint part, 7) shoulder protector plate.

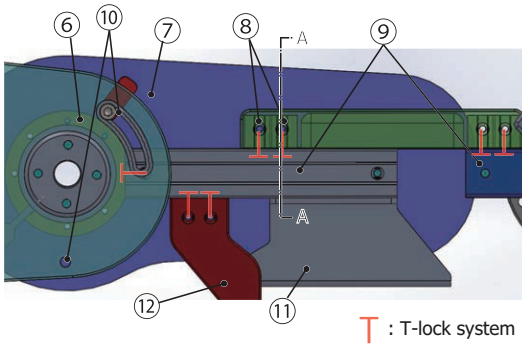

Fig. 3. Link adjustment structure, where a T-lock with a wedge screw connects the upper and lower frame rigidly (numbers continue from Fig. 2): 6) joint part, 7) shoulder protector plate, 8) holes of wedge screw for frame-length adjustment, 9) aluminum frames, 10) mechanical stopper (upper is adjustable), 11) arm rest plate attached to user's arm via brace, 12) part connected to pneumatic cylinder rod.

B. Adjustable exoskeleton frame with compact joint

Although an adjustable frame is an important element for comfortable use of an exoskeleton, the adjustment mechanisms tend to be large, not so rigid, and made with a complex structure. Therefore, a simple but sufficiently rigid connection is desirable for an adjustable system.

Fig.3 shows a CAD model of the adjustable frame around the shoulder joint and the link between the shoulder and elbow joints. The designed adjustable mechanisms have a

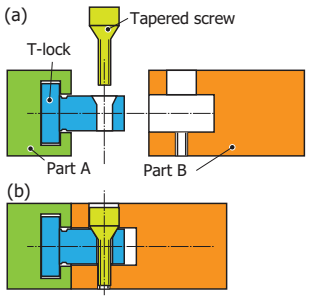

Fig. 4. T-Lock system: cross-sectional view corresponding to A-A in Fig. 3. The junction between two parts (Part A and Part B) is achieved by T-lock technology. The T-lock has a hole tapered at the top, and a tapered screw functions as a wedge connecting the two parts rigidly within a compact space.

compact and lightweight structure, but they can solidly fix the adjusted frame. This novel adjustable mechanism is based on a T-lock system, which is used as the connection component for a unique aluminum frame, called Recoframe (Yuki Laboratory Co., Ltd.). In Fig.3, part no. 9 is the off-the-shelf lightweight Recoframe (F152), and parts no. 6, no. 8, and no. 12 are custom-made using machining processes.

Fig.4 illustrates the T-lock system, corresponding to the cross-sectional view of A–A in Fig.3; it is composed of a T-lock and a wedge screw. This structure can be seen in classical Japanese carpentry, i.e., where two or more wooden parts are connected without using nails. In particular, we propose a novel way of using this locking structure for link adjustment. Without a tab in part B over part A, the screw can be inserted from the top (vertically), which is perpendicular to the conventional horizontal direction. Therefore, the tool used to loosen and tighten the screw can access the connection from the sagittal plane. Consequently, the frame can be easily adjusted.

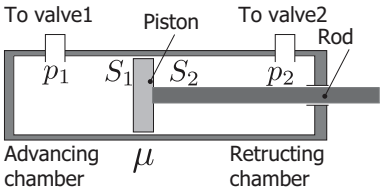

Fig. 5. Model of the piston: the pneumatic pressures in the advancing chamber and the retracting chamber are controlled independently.

C. Torque-based controller

Flow control valves to drive pneumatic actuators have been widely used, and several previous studies examined system identification methods for the flow-control valves[13][14][15][16]. On the other hand, recently, pressure servo valves with a built-in pressure controller, called a proportional pressure regulator, have become commercially available. Since the air pressure for the pneumatic actuators can be stably controlled by the proportional pressure regulators, we can control the joint torque of the exoskeleton

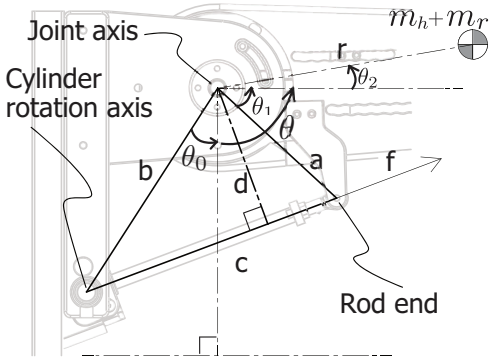

Fig. 6. Geometric model of effective moment arm of the pneumatic cylinder rod.

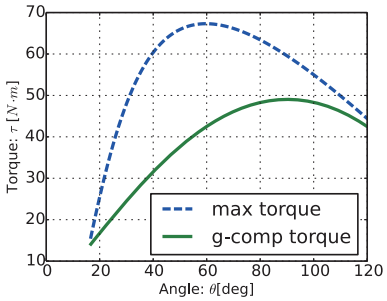

Fig. 7. Comparison of theoretical maximum torque and necessary torque for gravity compensation: maximum torque is the plot of shoulder elevation at 0.6 MPa; gravity-compensation torque is calculated from a 10 kg weight, which has a center of mass at 0.5 m from the shoulder's rotational axis.

robot by deriving the corresponding desired pressures for the pneumatic cylinder chambers.

Fig. 5 shows the model of the pneumatic cylinder and the piston. The shoulder torque for elevation (flexion-extension) is provided by force f applied to the cylinder rod, e.g., the differential of the pressures filling the cylinder chamber.

$$\tau = df, \tag{1}$$
$$f = \mu\left(S_1 p_1 - S_2 p_2\right), \tag{2}$$

where S_1 and p_1 are the space and the pressure of the advancing piston, and S_2 and p_1 are those of the retracting piston. d is the effective moment arm of the cylinder rod. Based on the law of cosines,

$$d = b\sin\left(\arccos\left(\frac{b^2+c^2-a^2}{2bc}\right)\right), \tag{3}$$

where c is the variable distance between the axis of the cylinder pivot and the tip of the axis (in our case, the rod end). a represents the distance between the cylinder rod end and the joint axis. On the other hand, b denotes the distance between the cylinder rotation axis and the joint axis. This length c can be measured using a linear encoder. If only a rotational encoder at the joint is available, c can be derived as

$$c = \sqrt{a^2+b^2-2ab\cos\left(\theta_0+\theta-\theta_1\right)}, \tag{4}$$

where θ is measured joint angle, and θ_0 and θ_1 are depicted in Fig. 6.

When τ^* is desired torque, the desired pressure p_1^*) or p_2^*, are provided:

$$p_1^* = \frac{\left(\frac{d\tau^*}{\mu} + p_2 S_2\right)}{S_1} \quad (\text{if } 0 \leq \tau^*) \tag{5}$$

$$p_2^* = - \frac{\left(\frac{d\tau^*}{\mu} - p_1 S_1\right)}{S_2} \quad (\text{if } \tau^* < 0). \tag{6}$$

Note that redundancy remains the pressure of the antagonistic chamber. In this paper's experiment, we set the desired pressures to the antagonistic chamber in the implementation. Assuming the elbow flexion-extension is fixed, the desired torque to achieve gravity compensation of the user's arm and the exoskeleton arm can be derived as:

$$\tau^* = (m_r + m_h)\, g r \sin(\theta + \theta_2), \tag{7}$$

where θ_2 is the elevation angle of the center of the arm from the link and r is the distance from the joint axis to the center of mass of the entire arm.

Fig.7 compares the theoretical maximum torque of the system and the necessary torque for gravity compensation. The gravity-compensation torque is calculated for the case where a 10 kg weight is placed at 0.5 m effective momentum arm. As of now, the designed mechanical range of the joint is $\theta \in [16.7, 120]$ deg. As seen in the figure, while there is a drop of the torque at the bottom of the angle, the maximum torque is sufficiently larger than the torque necessary for gravity compensation. Note that this torque range is large enough to actively moves typical human arm because the total weight of the arm is usually much lighter than 10 kg and the center of the mass locate shorter than 0.5 m.

III. Experiments

A. Experimental setup

1) Experimental task: Fig.8 shows the setup for the experimental task. To validate the design of the upper-extremity exoskeleton, the goal of the task is to power an attached passive mannequin arm as a dummy weight (1.65 kg). Since no actuator was installed on the mannequin arm, the task of actuating the sum of the exoskeleton arm and the mannequin arm inertia/mass can validate whether the prototyped exoskeleton can fully compensate the shoulder joint elevation (in both up/down directions).

The weight of the prototyped exoskeleton was 5.0 kg, including the 1-DOF active and 3-DOF passive joints but excluding the weight of the chair. The two braces as physical interfaces at the shoulder-elbow and elbow-wrist links softly couple the exoskeleton robot and the user's arm. Note that while the mannequin's elbow is a passive joint, the exoskeleton's elbow can fix it at different postures.

2) Controller unit: Fig.9 shows the valve control unit with a real-time PC for control. A laptop with a 14-inch screen, used as a terminal, is shown in the picture for size comparison. Internally, it has two valves (proportional pressure regulator: VP50, Norgren Co., Ltd.) and a load-cell amp, as well as a custom-made multifunction interface board (MFB) with analog-digital/digital-analog converters, input-output (IO), and a quadrature encoder interface (QEI) as a multi-interface to the valve, load cell, emergency switch cortex-M3 ARM core with 100-Mbps Ethernet port communicating with real-time PC (OS: Debian 7.4 with Xenomai Patch, *https://xenomai.org/*) through a real-time ethernet (RT-Net, *http://www.rtnet.org/*) TCP/IP (UDP) driver on an Intel e1000e ethernet controller. The built-in interpolator on the optical encoder (at chip level) and the quadrature encoder interface at the reading of encoded pulse (at the MBF side) are both set $\times 4$. Consequently, the theoretical resolution of the angle reading was $\times 16$ of the built-in scale, e.g. 0.025 deg (16000 CPR). For additional safety in case of emergency, the pneumatic output can be shut down by gating the power input to the valves. All of the interfaces and controllers are contained in half the volume of a 35-L suitcase for easy carrying, except for the oil-free scroll compressor (0.8 MPa Max, SLP-07EED, Anestiwata Co., Ltd.) that provides silent pneumatic generation behind the controller unit (nominal noise: 45 db).

3) Controller implementation: All of the controller implementation is done by python scripting on top of the C-embedded interface to real-time system calls. This enables the scripting language directory to be run in a real-time loop. The frequency of the control loop is set at 250 Hz. This is adequate for controlling the pneumatic servo system. Fig.10 shows the final implementation of the controller. In the lowest loop, the torque-based controller implements Eqs. (5) and (6) to control the open-loop pressure input to the proportional pressure regulator. This controller is used during direct teaching. In addition to the baseline of the gravity-compensation torque of (7), the PD controller provides the active movement torque.

Fig.11 (a) shows the angle trajectory observed in the gravity-compensation task as a direct-teaching interface (blue dashed line) and playback of the trajectory (green line). Fig.11 (b) shows the sequences of the gravity-compensation task in the direct-teaching phase. Since the gravity torque was successively generated, while the observed joint angle was maintained after release, the total mass/inertia of both the exoskeleton and the mannequin arm can be moved upward/downward with the small force produced by a single finger of the experimenter. This indicates the active joint is back-drivable and can compensate the entire torque to drive the mannequin arm and the exoskeleton arm. The assistive torque can be adjusted by decreasing the gain of the torque controller.

4) Physical Slider Interface: The PSI is implemented using a linear fader controller (iCONTROL PRO, iCon Co.,

Ltd.), which is typically used to control the fading of music volume by a disk jockey. These controllers are typically low cost and off-the-shelf products. However, to the best of the authors' knowledge, no project utilizes these types of mini interface for controller of. The midi-interface of the Pygame midi module, all of the slider's positions can be controlled/sensed via a built-in linear-positioning motor/sensor system, which syncs the slider position with a GUI (Fig.12 (a)). Another experiment showed how the PSI was used to control the exoskeleton prototype. This is the first trial, to the authors' best knowledge, of implementing such a slider interface as the control interface for a robotic arm.

5) Demonstration of major hardware characteristics: To validate whether the rigidity of the link-adjustable exoskeleton arm is enough high, the attached multimedia file also shows an experiment on a large-torque operation, in which the desired torque is gradually increased from 0 Nm to 50 Nm and the experimenter tries to apply resistance to the mannequin arm's elevation. This and the above experiments can be viewed from the multimedia attachment in several movie scenes: #1: Physical Slider Interface, #2: Direct teaching with gravity compensation, #3: Playback, #4 Fix/release elbow joint, #5: Ramp signal input to torque based-controller for shoulder joint (0–50 Nm).

IV. Conclusion

This article presented the newly developed upper-extremity exoskeleton in which a 1-DOF active joint actuated by a pneumatic cylinder and 3-DOF passive joints are implemented for adjusting arm posture in a rehabilitation setting. The design of the developed hardware was based on a compact joint and a link length that is adjustable and rigid. These features were powered by the technologies of a high-resolution, built-in encoder on a thrust bearing and an adjustable frame with a wedge structure. Accordingly, the prototype is enough strong to transmit the large torque generated from the pneumatic cylinder.

The gravity compensation implemented on the torque-based controller was demonstrated, and we found that it only took one finger to easily rotate the total mass of a mannequin's dummy weight and the exoskeleton frame in the up/down direction, and the device kept its posture after release. This system can be used for direct teaching of motion control while the patient's arm is attached to the exoskeleton. From the playback experiment, using a PD controller on top of the torque-based controller, we found that the proposed technique sufficiently drives the total mass/inertia of the exoskeleton and mannequin arm.

The developed shoulder exoskeleton platform was designed to generating enough large torque to actively move resisting to stiff shoulder due to spasms. Current implementation of additional safety is emergency button and mechanical stoppers at bottom and top. While the active joint is back-drivable in hardware level, torque limitation at the torque-based controller has to be taken into consideration for a patient study. Future work includes further development of the controller for further assured safety and user interfaces for better safety in human-subject studies.

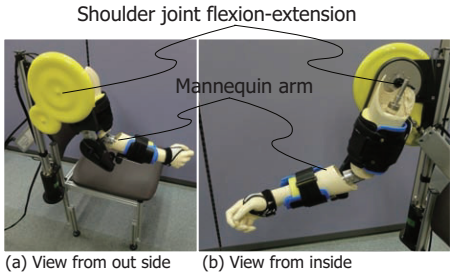

Fig. 8. Experimental setup: A mannequin arm is attached to the upper-extremity exoskeleton as a dummy weight.

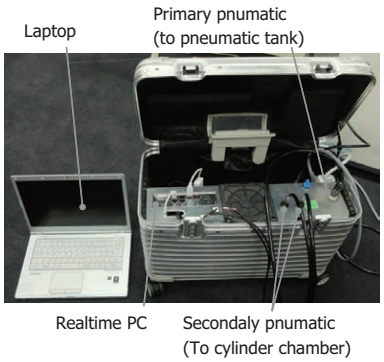

Fig. 9. Control unit with valves, load-cell amp, multifunction interface board (ADC/DAC/IO/QEI interfaces), and real-time control PC all installed within half the volume of a small suitcase.

Acknowledgements

We thank Prof. Liu Meigen, Dr. Katsuhiro Mizuno, Dr. Junichi Ushiba, and Dr. Shoko Kasuga of Keio University for advising us on the development of the upper-extremity exoskeleton. Dr. Asuka Takai and Dr. Tatsuya Teramae helped the development of Physical Slider UI. Mr. Nao Nakano, and Mr. Akihide Inano helped us with hardware maintenance in the experimental setup. A part of the research was supported by "Development of BMI Technologies for Clinical Application" carried out under SRPBS by the MEXT/AMED, a contract with the Ministry of Internal Affairs and Communications entitled, "Novel and innovative R&D making use of brain structures.", ImPACT Program of Council for Science, Technology and Innovation (Cabinet Office, Government of Japan), a project commissioned by the NEDO, and MIC-SCOPE. T.N. was partially supported by JSPS KAKENHI 15H05321, 24700203, and 26540134, and by Tateisi Science and Technology Foundation. J.M. was partially supported by JST-SICP and MEXT KAKENHI 23120004.

References

[1] S. S. Virani, N. D. Wong, D. Woo, M. B. Turner, and S. S. Stroke, "Heart disease and stroke statistics–2014 update: a report from the... - PubMed - NCBI," *Circulation*, 2014.

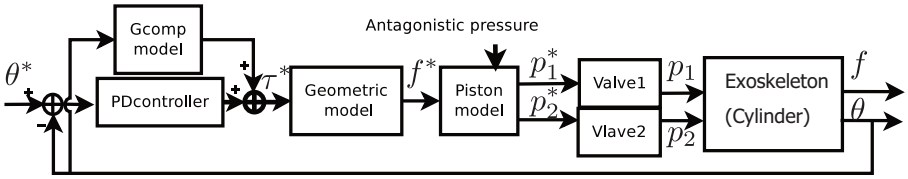

Fig. 10. Block diagram of controller implementation

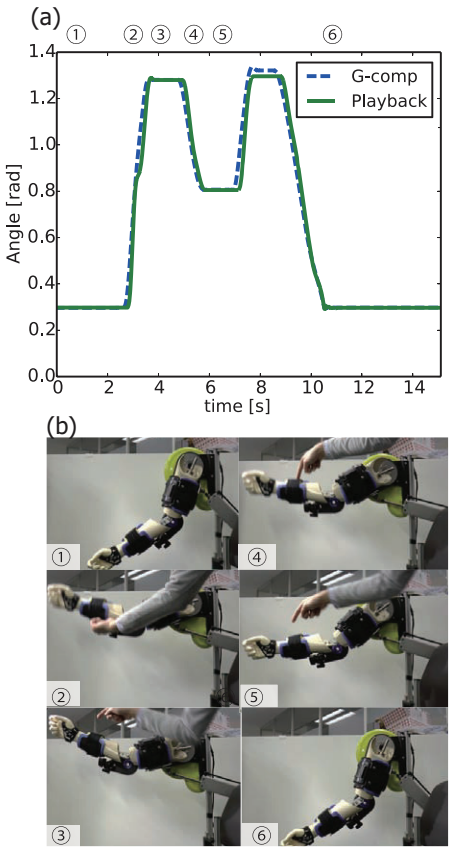

Fig. 11. Gravity compensation task: the exoskeleton drives the shoulder joint with a mannequin arm as dummy weight using a gravity-compensation torque. (a) Dashed plot shows the angle trajectory during gravity compensation, and solid green line shows the playback experiment using a PD controller on top of the torque-based controller. (b 1–6) (1) Initial posture; (2) Arms can be moved upward using one finger; (3) Exoskeleton kept its posture after release; (4) Moving downward; (5) Exoskeleton kept its posture after release in a different posture than (4); and (6) final posture.

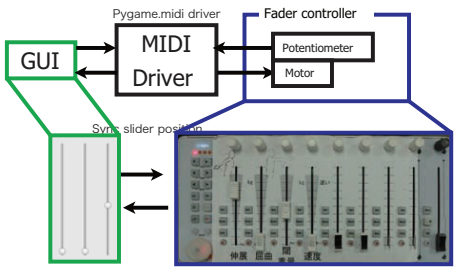

Fig. 12. Physical slider user interface: Through the MIDI driver, the fader positions are synchronized with the positions of the GUI slider.

[2] T. Nef, M. Guidali, and R. Riener, "ARMin III – arm therapy exoskeleton with an ergonomic shoulder actuation," *Applied Bionics and Biomechanics*, vol. 6, no. 2, pp. 127–142, Jul. 2009.

[3] H. Vallery, J. Veneman, E. van Asseldonk, R. Ekkelenkamp, M. Buss, and H. van Der Kooij, "Compliant actuation of rehabilitation robots," *IEEE Robotics and Automation Magazine*, vol. 15, no. 3, pp. 60–69.

[4] K. KIGUCHI, "Active exoskeletons for upper-limb motion assist," *International Journal of Humanoid Robotics*, vol. 4, no. 03, pp. 607–624, 2007.

[5] J. F. Veneman, R. Kruidhof, E. E. G. Hekman, R. Ekkelenkamp, E. H. F. Van Asseldonk, and H. van der Kooij, "Design and Evaluation of the LOPES Exoskeleton Robot for Interactive Gait Rehabilitation," *IEEE Trans. Neural Syst. Rehabil. Eng.*, vol. 15, no. 3, pp. 379–386.

[6] H. Kazerooni, "That which does not stabilize, will only make us stronger," in *Rehabilitation Robotics, 2007. ICORR 2007. IEEE 10th International Conference on*, 2007, p. 18.

[7] D. G. Caldwell, N. G. Tsagarakis, S. Kousidou, N. Costa, and I. Sarakoglou, "Soft exoskeletons for upper and lower body rehabilitation – design, control and testing," *International Journal of Humanoid Robotics*, vol. 04, no. 03, pp. 549–573, 2007.

[8] E. T. Wolbrecht, D. J. Reinkensmeyer, and J. E. Bobrow, "Pneumatic Control of Robots for Rehabilitation," *The International Journal of Robotics Research*, vol. 29, no. 1, pp. 23–38, Jan. 2010.

[9] M. Takaiwa and T. Noritsugu, "Development of wrist rehabilitation equipment using pneumatic parallel manipulator," pp. 2302–2307, 2005.

[10] H. Kobayashi, A. Takamitsu, and T. Hashimoto, "Muscle Suit Development and Factory Application," *International Journal of Automation Technology*, vol. 3, no. 6, pp. 709–715.

[11] T. Tsuji, C. Momiki, and S. Sakaino, "Stiffness control of a pneumatic rehabilitation robot for exercise therapy with multiple stages," in *Intelligent Robots and Systems (IROS), 2013 IEEE/RSJ International Conference on*, 2013, pp. 1480–1485.

[12] T. Noda, T. Teramae, B. Ugurlu, and J. Morimoto, "Development of an upper limb exoskeleton powered via pneumatic electric hybrid actuators with bowden cable," in *Intelligent Robots and Systems (IROS 2014), 2014 IEEE/RSJ International Conference on*, Sept 2014, pp. 3573–3578.

[13] J. E. Bobrow and B. W. McDonell, "Modeling, identification, and control of a pneumatically actuated, force controllable robot," *Robotics and Automation, IEEE Transactions on*, vol. 14, no. 5, pp. 732–742, 1998.

[14] N. Gulati and E. J. Barth, "A Globally Stable, Load-Independent Pressure Observer for the Servo Control of Pneumatic Actuators," *Mechatronics, IEEE/ASME Transactions on*, vol. 14, no. 3, pp. 295–306, 2009.

[15] ——, "Non-linear pressure observer design for pneumatic actuators," in *Advanced Intelligent Mechatronics. Proceedings, 2005 IEEE/ASME International Conference on*, 2005, pp. 783–788.

[16] Y. Tassa, T. Wu, J. Movellan, and E. Todorov, "Modeling and identification of pneumatic actuators," in *Mechatronics and Automation (ICMA), 2013 IEEE International Conference on*, 2013, pp. 437–443.